A Control System for a Flexible Spine Belly-Dancing Humanoid

Jimmy Or
Takanishi Laboratory
Humanoid Robotics Institute
Waseda University
#59-308, 3-4-1 Ookubo
Shinjuku-ku
Tokyo, Japan 169-8555
jimmyor@kurenai.waseda.jp

Abstract Recently, there has been a lot of interest in building anthropomorphic robots. Research on humanoid robotics has focused on the control of manipulators and walking machines. The contributions of the torso towards ordinary movements (such as walking, dancing, attracting mates, and maintaining balance) have been neglected by almost all humanoid robotic researchers. We believe that the next generation of humanoid robots will incorporate a flexible spine in the torso. To meet the challenge of controlling this kind of high-degree-of-freedom robot, a new control architecture is necessary. Inspired by the rhythmic movements commonly exhibited in lamprey locomotion as well as belly dancing, we designed a controller for a simulated belly-dancing robot using the lamprey central pattern generator. Experimental results show that the proposed lamprey central pattern generator module could potentially generate plausible output patterns, which could be used for all the possible spine motions with minimized control parameters. For instance, in the case of planar spine motions, only three input parameters are required. Using our controller, the simulated robot is able to perform complex torso movements commonly seen in belly dancing as well. Our work suggests that the proposed controller can potentially be a suitable controller for a high-degree-of-freedom, flexible spine humanoid robot. Furthermore, it allows us to gain a better understanding of belly dancing by synthesis.

Keywords
Next generation high-degree-of-freedom flexible spine humanoid robot, belly dancing, lamprey central pattern generator, neural networks, robot controller, motor primitives

1 Introduction

Recently, there has been much interest in anthropomorphic robots [5, 2, 15, 29, 31, 32, 24, 25]. Research on humanoid robots concentrates on three areas: control of manipulators, biped locomotion, and human-robot interaction.

Over the past 30 years, a lot of walking machines have been created, because only a small percentage of the world is accessible by wheels. Although recently developed robots (such as the Sony SDR-4, Fujitsu HOAP-1, and Honda ASIMO) are able to walk and climb stairs, their movements are not natural looking. A common feature of these robots is a rigid torso. So far, the interactions between body posture and leg movement during locomotion have been neglected by almost all humanoid robotics researchers. In order to walk like a human, it is necessary for the robot to have a flexible body trunk and hip.

Research on human-robot interaction is a relatively new field. Some researchers are using head robots to communicate with humans [16, 4, 23]. Others are trying to find a simpler way to teach

robots complex motor skills by imitation learning [2, 3, 18, 22]. Although a few recently developed head robots are capable of communicating with humans through speech and facial expressions, the communication is not very natural, because body language is not involved. For this it would be necessary to equip these robots with a pair of limbs and a flexible torso.

Similar to snakelike robots such as the ones proposed in [6, 30, 21] and the tendon driven robots described in [24, 25], the next generation of humanoid robots will incorporate a flexible spine as the torso.[1] Given that such a robot will have a greater degree of freedom (DOF) than existing robots, it is necessary to find a simple control strategy to cope with the increased complexity. Inspired by the rhythmic movements commonly seen in lamprey locomotion as well as belly dancing, we designed a controller for a simulated belly-dancing robot based on the lamprey central pattern generator (CPG).

According to Grillner [12], the lamprey belongs to the most primitive vertebrate group, the *cyclostomes*. Its evolution diverged from the main vertebrate line about 450 million years ago. It is considered by biologists to be a *prototype vertebrate* because its brain stem[2] and spinal cord have all the basic vertebrate features, yet the neurons in each category are an order of magnitude fewer than in other vertebrates [13]. The lamprey swimming circuitry has therefore been studied extensively by neurobiologists who want to understand the principles underlying vertebrate (such as human) locomotion [12]. We believe that some of the principles found in the motor control of the lamprey can be applied to the design of a controller for a high-DOF humanoid robot. The reason is that the lamprey has 100 segments, each of which has at least four muscles (to allow yaw, pitch, and roll). By varying only the global and extra excitations from the brain stem, the lamprey is able to change its body shape. Such simplicity is ideal in a controller for a high-DOF, flexible spine humanoid robot. As a first step, we investigate the possibility of using a CPG-based controller and a minimized number of input parameters to control a high-DOF, flexible spine model humanoid.

Belly dancing was chosen as a motor task for the following reasons. First, belly dancers have very flexible bodies. They can bend their arms, legs, and torso more smoothly than an average person. Robots, on the other hand, have rigid torsos and tend to produce jerky movements. Secondly, belly dancers are able to maintain good balance, a quality that is very important for humanoid robots. If a robot were as flexible as a belly dancer, it could perform tasks that no robot has done before. For instance, it would generally be more agile, more able to work its way through tight spaces, and perhaps able to climb steep inclines using hand- and footholds. It could also step over clutter and walk naturally (or perhaps even jump) using sparse footholds. Other benefits would include walking naturally, swimming efficiently, balancing, and playing golf. Belly dancing is also interesting from a control point of view. The basic steps are rhythmic and often involve traveling waves along the torso and arms. Movements with these features can easily be generated by the lamprey CPG with no more than three control parameters. They can also be extracted as motor primitives for a robot to learn complex motor tasks through imitation learning. Finally, the study of traveling waves is important to motor control because this kind of body undulation has been observed in other animals (such as anguilliform swimmers, salamanders, and cats) during locomotion.

1 In Mizuuchi et al. [24, 25], the authors presented two interesting flexible spine humanoid robots. But there are as yet no experimental data to support their claims about the capabilities of these robots.

2 According to Grillner et al. [14], the lamprey brain stem consists of four different reticular nuclei. The most rostral nucleus is located in the mesencephalon (MRN), and the rest of the nuclei are in the rhombencephalon: the anterior (ARRN), the middle (MRRN), and the posterior (PRRN). Some of these reticulospinal neurons are active tonically, while others receive feedback from the spinal cord that results in phasic modulation. The glutamatergic reticulospinal MRRN and PRRN neurons project to the spinal cord and are responsible for the initiation of locomotion. These neurons can be activated from the rostral brain stem structures and other sensory stimuli. Upon activation, these reticulospinal cells in turn activate the AMPA/kainate- and NMDA-type glutamate receptors located on the spinal cells of the locomotion CPGs to initiate locomotion. Note that the level of activity of the CPGs is controlled by the reticulospinal neurons. The higher the level of activity in these neurons, the faster the animal moves. In our implementation, the brain stem itself is considered as a neuron unit.

2 Background

2.1 Belly Dance

According to Atéa [1],

> "Belly dance" consists of a movement vocabulary that sets it apart from any other dance form. Its most distinguishing feature is its isolated movements of the abdomen. These abdominal movements may be circular, rolling, angular, or vibrating, and are unique to this dance. But belly dance is a form that involves every other part of the body too, isolating major muscle groups and working them in isolation or in opposition to other parts of the body. Other distinguishing features are circular or wavelike moves of arms, hands, upper torso, and hips.

For over 2000 years, this dance form has been practiced for the relief of back pain, childbirth preparation, physical education, entertainment, and ritual [1]. Although it is common to see male belly dancers in the Middle East countries, in other parts of the world belly dancing is mainly performed by females. The main benefits of belly dancing is that it is good for the muscles used during labor and delivery. The rhythmic movements are beneficial to pregnant women.

Some belly-dance moves, such as the *camel*, require independent control of muscle groups and coordination between body segments. Typically, only advanced dancers are able to propagate a traveling wave along their bodies with ease. Since we are interested in the control of flexible spine humanoid robots, we focus on the torso movements in this article. For more details on belly dancing, refer to [1, 27].

2.2 The Human Spine

The human spine is an arched vertebral column. It consists of seven cervical vertebrae, twelve thoracic vertebrae, five lumbar vertebrae, the coccyx, and the sacrum. Between each neighboring pair of vertebrae there is an intervertebral disk, which acts as a shock-absorbing cushion (Figure 1). The actions that are possible in the three spinal regions (cervical, thoracic, and lumbar) on the sagittal, frontal, and transverse planes[3] depend on the different sizes, shapes, and articulations of the bones [10]. According to kinesiologists such as Fitt, the possible actions achieved by the human spine are:

1. *Flexion* and *hyperextension* on the sagittal plane.
2. *Lateral flexion* to either side of the body on the frontal plane.
3. *Rotation* to the left and right on the transverse plane. This is mainly achieved in the thoracic region.

The main functions of the spine are to protect the spinal cord and to act as a support to the upper body weight. In addition, it provides both stability and mobility in our daily activities. The last two functions are very important for flexible spine humanoid robots.

3 Neural Model of the Lamprey CPG

A connectionist model of the lamprey CPG has been handcrafted based on findings from physiological experiments [9]. In this model the entire network consists of 100 interconnected

3 *Sagittal plane*: a vertical plane extending front to back that divides the body into right and left parts. *Frontal plane*: a vertical plane extending side to side that divides the body into front and back parts. *Transverse plane*: a horizontal plane extending side to side and front to back that divides the body into upper and lower parts. Each kind of plane is perpendicular to the other two.

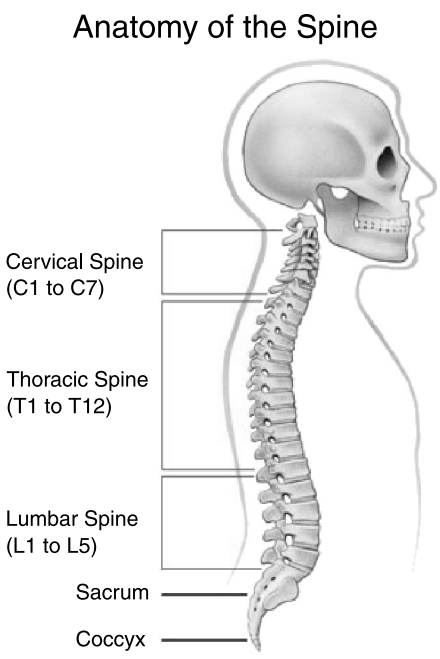

Figure 1. The human spine. (Illustrated by Jim Shea. Modified with permission.)

copies of a segmental oscillator (Figure 2). Within each segmental oscillator, there are eight neuron units of four types, namely motoneurons (MN), excitatory interneurons (EIN), contralateral inhibitory interneurons (CIN), and lateral inhibitory interneurons (LIN). Each of these units represents a population of functionally similar neurons in the real lamprey. They all receive excitations from the lamprey brain stem.

Since the details of the intersegmental connections of the real lamprey CPG are not yet known, Ekeberg [9] simplified the controller by giving each neuron symmetrical connections extending in both rostral and caudal directions (except for the CIN neurons, which have longer projections in the caudal direction). Given that the neurons at both ends of the CPG receive fewer neural connections, synaptic weights are calibrated by dividing them by the number of segments a neuron receives input from. The connection weights among the neurons are given in Table 1.

Using the given neural couplings, we are able to control the intersegmental phase lag by varying only the amount of extra excitation from the brain stem. Furthermore, the frequency of segmental oscillations (which affects the speed of locomotion) and intersegmental phase lag (which affects the body shape) can be controlled almost independently (Section 3.5).

3.1 Mathematical Model of Neurons

To model a neuron unit, we used a leaky integrator with a saturating transfer function. The output u ($\in [0, 1]$) of the unit neuron is the mean firing frequency of the population it represents. It is calculated using the following set of formulas:

$$\dot{\xi}_+ = \frac{1}{\tau_D}\left(\sum_{i\in\Psi_+} u_i w_i - \xi_+\right), \tag{1}$$

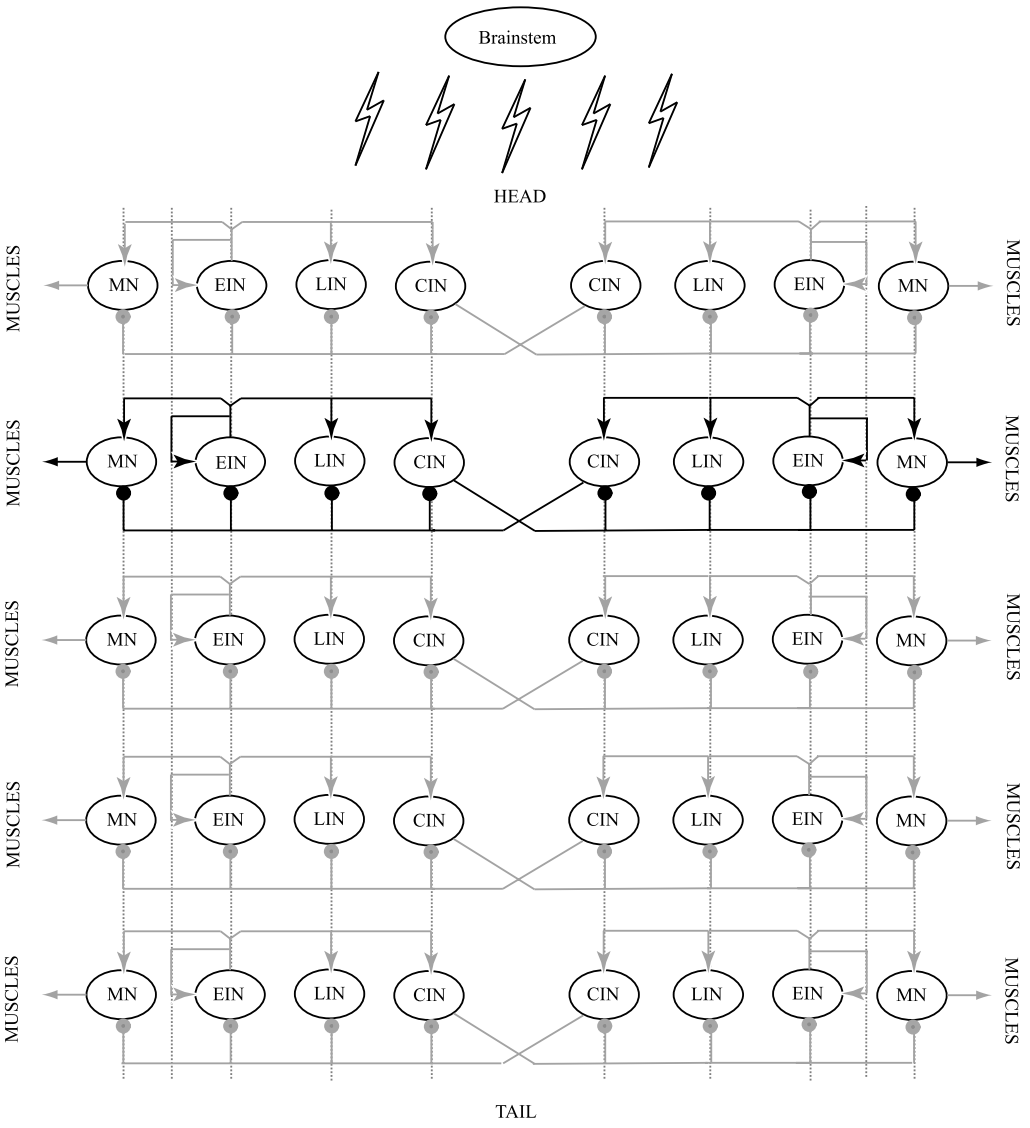

Figure 2. Configuration of the lamprey CPG. The controller is composed of 100 interconnected segmental oscillators (only five segments are shown here). Each segment consists of eight neurons of four types: motoneurons (MN), excitatory interneurons (EIN), lateral inhibitory interneurons (LIN), and contralateral inhibitory interneurons (CIN). Connections with a fork ending represent excitatory connections, while those with a dot ending represent inhibitory connections. Vertical lines indicate that there are intersegmental couplings among the neurons within the CPG. Due to the complexity of the couplings, the actual intersegmental connections are not shown here. (Refer to Table 1 for details.) Note that in our implementation, the brain stem itself is considered as a neuron unit. Each neuron within the CPG receives the same amount of global excitation from this special neuron. Moreover, neurons near the head segments receive extra excitation. In addition to input signals from the brainstem, the controller receives feedback from the stretch sensitive edge EC cells. Note that these cells are not implemented in the current controller.

Table 1. Connection weight matrix for the lamprey CPG [9]. Excitatory and inhibitory connections are represented by positive and negative weights respectively. Left and right neurons are indicated by l and r. BS stands for brain stem. The extensions from a neuron to those in neighboring segments are given in brackets. The first number is the number of extensions in the rostral direction; the second, in the caudal direction.

To:	From: EINl	CINl	LINl	EINr	CINr	LINr	BS
EINl	0.4 [2, 2]	—	—	—	−2.0 [1, 10]	—	2.0
CINl	3.0 [2, 2]	—	−1.0 [5, 5]	—	−2.0 [1, 10]	—	7.0
LINl	13.0 [5, 5]	—	—	—	−1.0 [1, 10]	—	5.0
MNl	1.0 [5, 5]	—	—	—	−2.0 [5, 5]	—	5.0
EINr	—	−2.0 [1, 10]	—	0.4 [2, 2]	—	—	2.0
CINr	—	−2.0 [1, 10]	—	3.0 [2, 2]	—	−1.0 [5, 5]	7.0
LINr	—	−1.0 [1, 10]	—	13.0 [5, 5]	—	—	5.0
MNr	—	−2.0 [5, 5]	—	1.0 [5, 5]	—	—	5.0

$$\dot{\xi}_- = \frac{1}{\tau_D}\left(\sum_{i\in\Psi_-} u_i w_i - \xi_-\right), \tag{2}$$

$$\dot{\vartheta} = \frac{1}{\tau_A}(u - \vartheta), \tag{3}$$

$$u = \begin{cases} 1 - \exp\{(\Theta - \xi_+)\Gamma\} - \xi_- - \mu\vartheta & (u > 0), \\ 0 & (u \le 0) \end{cases} \tag{4}$$

where w_i represents the calibrated synaptic weights, and Ψ_+ and Ψ_- represent the groups of presynaptic excitatory and inhibitory neurons, respectively. ξ_+ and ξ_- are the delayed reactions to excitatory and inhibitory inputs, and ϑ represents the frequency adaptation[4] observed in real neurons [9]. Note that since the function of the brain stem is to excite the neurons in the CPG network, one of the u_i inputs in Equation 1 is from the brain stem. Thus, the more excitations from the brain stem input, the more excited the neuron unit becomes and the higher the frequency of oscillation. To simulate extra excitations, connection weights from the brain stem to the neurons in the first five segments are amplified accordingly.

The parameters for each type of neuron are given in Table 2. The values of these parameters and those for the connection weights are set up in such a way that the simulation results from the model agree with physiological observations.

4 Frequency adaptation is a neural property. It means that the firing rate of a neuron is not constant for a constant input. Typically, there is a slight decrease in the firing rate over time.

Table 2. Neuron parameters. Θ is the threshold, Γ the gain, τ_D the time constant of the dendritic sums, μ the coefficient of frequency adaptation, and τ_A the time constant of frequency adaptation.

Neuron type	Θ	Γ	τ_D (ms)	μ	τ_A (ms)
EIN	−0.2	1.8	30	0.3	400
CIN	0.5	1.0	20	0.3	200
LIN	8.0	0.5	50	0.0	—
MN	0.1	0.3	20	0.0	—

To calculate the neural activity of the entire swimming controller, we integrate Equations 1 to 4 using a fourth-order Runge-Kutta (RK4) method with a fixed time step of 1 ms.

3.2 Behavior of a Segmental Oscillator

The behavior of a segmental oscillator can be described as follows (refer to the highlighted segment in Figure 2). The brain stem provides input signals to stimulate all the neurons. Only neurons that are actively inhibited stay inactive.

Suppose that initially the neurons on the left are slightly more active. The EINl neuron excites all the ipsilateral neurons, while the CINl neuron inhibits all the contralateral neurons. This prevents simultaneous activity on both sides. Due to its higher threshold and time constant (Table 2), the LINl neuron becomes active later in the cycle to act as a burst suppressor to the CINl neuron. This allows the neurons on the right to become active. The CINr neuron on the right in turn inhibits all the neurons on the left. After a while, the activities of the neurons on the right are terminated by the LINr neuron, and the entire cycle starts again. Using this mechanism, an alternating pattern of muscular activity on the right and left sides of a single body segment can be generated.

3.3 Behavior of the Entire Lamprey CPG

The complete lamprey CPG functions as follows. Global excitation from the brain stem stimulates all neurons in the CPG; sufficient stimulation results in oscillations in each individual segment at a frequency that depends on the strength of this global excitation signal. Extra excitation is supplied from the brain stem to the five most rostral segments of the CPG. The effect of this, interacting with intersegmental coupling, is to induce a roughly equal relative phase lag between successive segments in the CPG, with the result that caudally traveling waves of neural activity appear. The global excitation controls the amplitude (mean firing frequency) of the motoneuron outputs as well as the frequency of oscillation of the CPG. The extra excitation alters the intersegmental phase lag largely independently of the global excitation.

3.4 Quantitative Analysis of a Segmental Oscillator

A quantitative analysis of our implementation of Ekeberg's segmental oscillator model follows.

In order to determine how the segmental oscillator behaves under different excitations, we tested our implementation of Ekeberg's segmental oscillator with a brain stem excitation from 0.2 to 1.0 in steps of 0.1. For each excitation value, a neural simulation is performed. At the end of each simulation, the amplitude and frequency from the outputs of the left motoneurons are calculated. The outputs from each neuron over time can optionally be stored in a data file for visualization under MATLAB.

When the segmental oscillator with asymmetric initial conditions[5] receives enough excitation from the brain stem, an alternating pattern of neural activity is generated (see Figure 3).

5 ξ_+ (0) = 1 and ξ_- (0) = 0 for all the left neurons, and ξ_+ (0) = ξ_- (0) = 0 for all the right neurons.

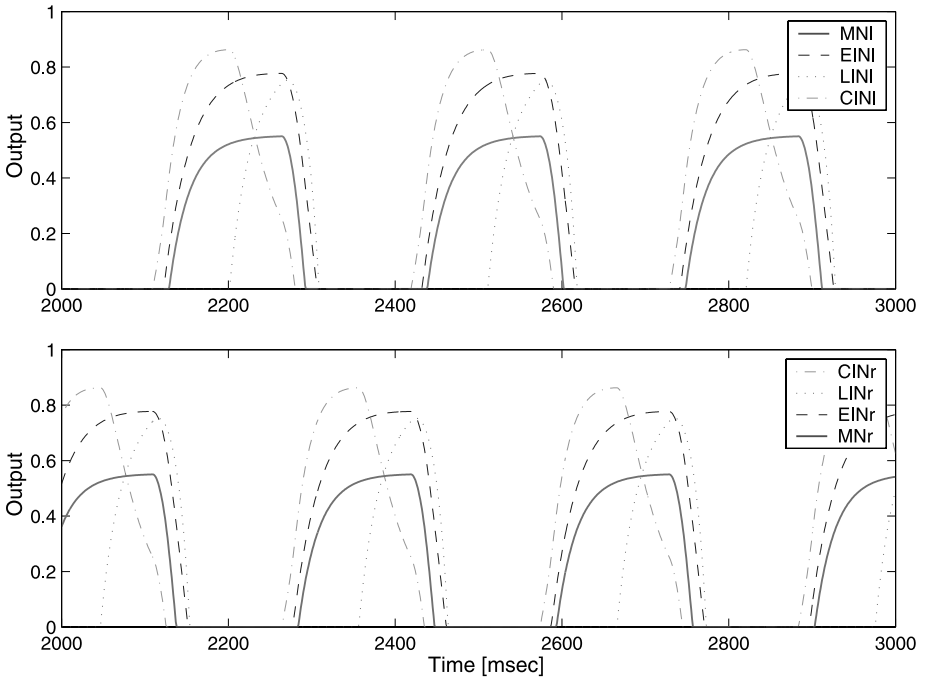

Figure 3. Output of neurons from a segmental oscillator with an excitation of 0.4.

Increasing the brain stem excitation from 0.2 to 1.0 increases the maximum amplitude as well as the frequency of oscillation of the motoneuron outputs. The amplitude ranges from 0.38 to 0.81, while the oscillation frequency ranges from 1.64 to 5.49 Hz (see Figure 4).

3.5 Quantitative Analysis of the Lamprey CPG

To determine how the entire CPG behaves under different excitation combinations, we tested our implementation of Ekeberg's model under global excitation ranges from 0.2 to 1.0 (in steps of 0.1) and extra excitation ranges from 0% to 200% (in steps of 10%). Recall that global excitation is the excitation that the brain stem applies to all the neurons in the CPG, and extra excitation is the excitation applied only to the neurons located in the five segments closest to the head. The extra excitation is a percentage of the global excitation. At each excitation combination, a neural simulation is performed. The characteristics (such as amplitude, frequency, and phase lag) of the neural wave that result from the outputs of the left motoneuron in the middle of the CPG, say segment 50, are recorded. The results are shown in Figure 5.

The amplitude surface shows that as the global excitation increases, the amplitude of the motoneuron outputs increase. The amplitude stays fairly constant when the extra excitation is increased. Similar to what we observe for the amplitude surface, the frequency surface shows that as the global excitation increases, the frequency of oscillation increases. Although there is a slight increase in frequency with extra excitation, the frequency stays fairly constant. On the other hand, the phase lag surface indicates that the phase lag increases with extra excitation but stays fairly constant with increase in global excitation. Note that the empty regions in all three surfaces correspond to quantities that cannot be measured. We consider the outputs from the motoneurons to be valid only when both the left and right signals oscillate and return to zero. The reason for this is that the time instants when pulse onsets appear are required in order to calculate the frequency and phase lag.

The frequency and phase lag surfaces show that the frequency of oscillation and the wavelength of undulation can be changed almost independently. Hence, just as in the real lamprey, the neural

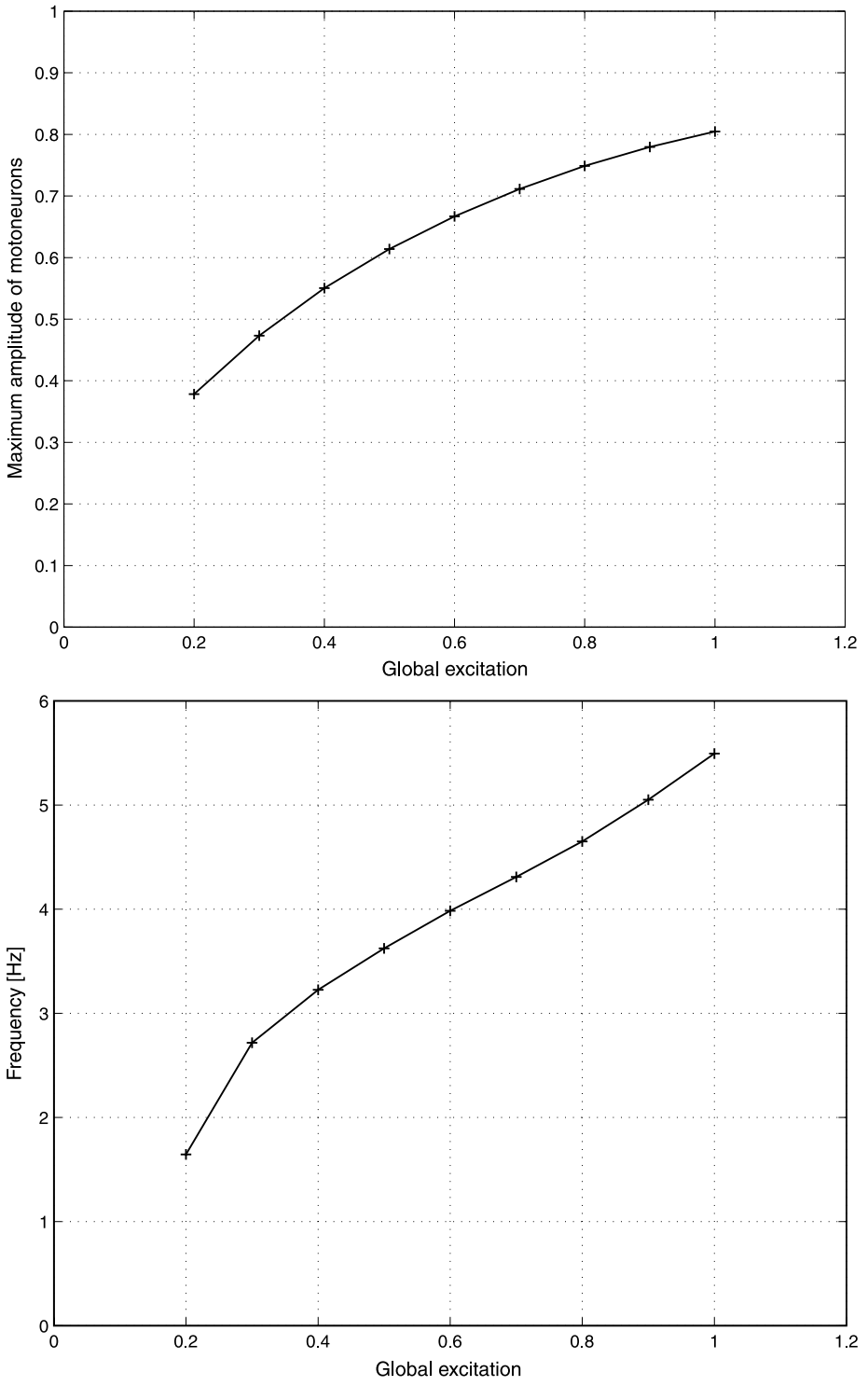

Figure 4. Effect of excitation from the brain stem on the amplitude of motoneuron output (*left*) and the frequency of oscillation (*right*) of the biological segmental oscillator.

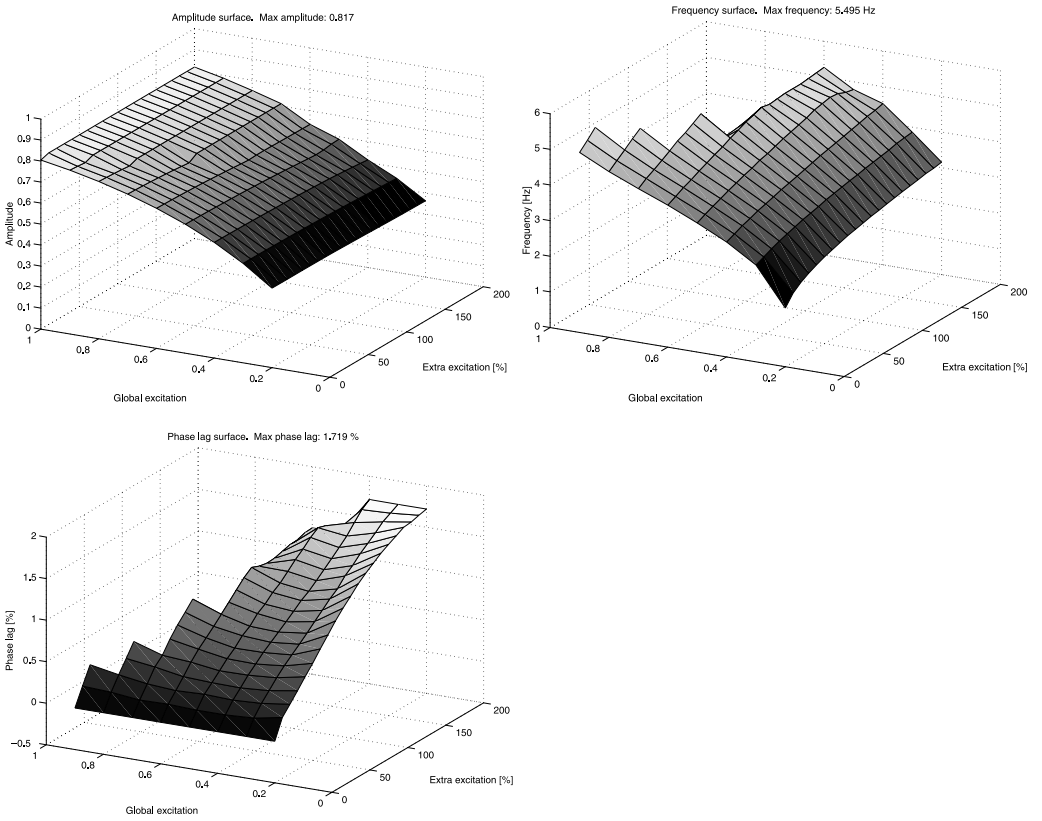

Figure 5. Effect of the global and extra excitations on the amplitude of motoneuron output (*top left*), the frequency of oscillation (*top right*), and the phase lag (*bottom*) of the lamprey CPG.

model is capable of producing a range of oscillation frequencies while keeping the wavelength of undulation constant.

4 Mechanical Model of the Humanoid

We simulated a belly-dancing humanoid in Poser 5 (Curious Labs), using the 3D human skeleton model developed by DAZ Productions. The reason for choosing this model is its similarity to a real skeleton: each of the individual vertebrae has a 3-DOF joint, which allows rotations along the yaw, pitch, and roll axes.[6] To rotate a joint about a specific axis, one can use the dials in the parameters palette or data from an external file. Another advantage of using the skeleton model is that it is easier to show body movements without clothing.

According to Kandel et al. [20],

> Dermatomes[7] are arranged in a highly ordered way on the body surface. It has been possible to map the distribution along the body surface of the dermatomes for all of the spinal segments by studying the sensibility and responsiveness that remain after injury to dorsal roots . . . dermatomal maps provide an important diagnostic tool for localizing levels of injury to the spinal cord and dorsal roots.

6 Note that the four basic spine motions and body undulations are planar motions. Once the plane of motions is specified, all the vertebrae turn about the same axis and the other degrees of freedom are fixed.

7 A *dermatome* is a restricted peripheral region of the skin. It is innervated by a single dorsal root, which contains sensory neurons that enter the spinal cord from the body.

Guided by the dermatomal maps (Figure 6), we coupled the motoneuron outputs from the lamprey CPG to the model spine (Table 3).

Given that each motoneuron output is between 0 and 1 (Section 3.1), the difference between the left and right motoneuron outputs at each segment is amplified 20 times. After this amplification, the spinal movements become observable and realistic. Each calibrated value is then used as the rotational angle (along a specific axis of rotation) for the corresponding vertebra. The effect of global excitation from the brain stem on the maximum rotational angle is shown in Figure 7.

5 Posture Database

In a typical course on belly dancing, the students learn a set of basic body postures, which forms the vocabulary of the dance. As the course progresses, more advanced dance movements can be accomplished by sequencing and/or superposing the basic postures. These postures are analogous to the *motor primitives* commonly described in literature on imitation learning [22, 19, 26].

As mentioned previously, the beauty of belly dancing is that the body motions are rhythmic and well defined. Most of the seemingly complex dance moves emerge from a combination of sliding, circulating, twisting, and wavelike moves of the torso and arms. Moreover, belly dancing requires only a small movement envelope compared with other dances. These features allow us to easily extract the trajectories of body segments without the use of expensive 3D motion capture systems.

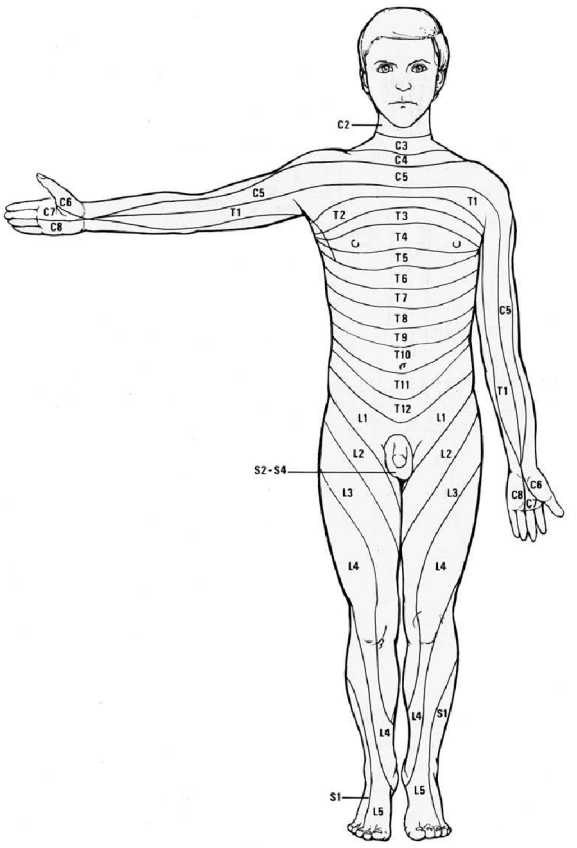

Figure 6. The dermatomes of each spinal segment are located on particular regions of the body: C, cervical; T, thoracic; L, lumbar; S, sacral [20].

Table 3. Mapping from the neural segments to the model spinal vertebrae: C, cervical; T, thoracic; L, lumbar. The reason we do not use vertebrae C1 to C3 is that they function more as part of the head than of the neck. Refer to Figure 1 for more details on the anatomy of the spine.

Spinal region	Vertebra	Neural segment
Cervical	C4	1
	C5	5
	C6	10
	C7	15
Thoracic	T1	20
	T2	25
	T3	30
	T4	35
	T5	40
	T6	45
	T7	50
	T8	55
	T9	60
	T10	65
	T11	70
	T12	75
Lumbar	L1	80
	L2	85
	L3	90
	L4	95
	L5	100

Through computer animations and immediate feedback from a professional dance teacher, we developed a database of belly dance movements. It contains a set of fundamental dance postures (Figure 8).

By sequencing these basic building blocks, more complex dance movements can be reproduced. Our analysis shows that four types of articulations are involved in belly dancing (Figure 9). A set of actuators which can produce the motions in (a) and (b) can be used for the control of a real belly dancing humanoid robot.

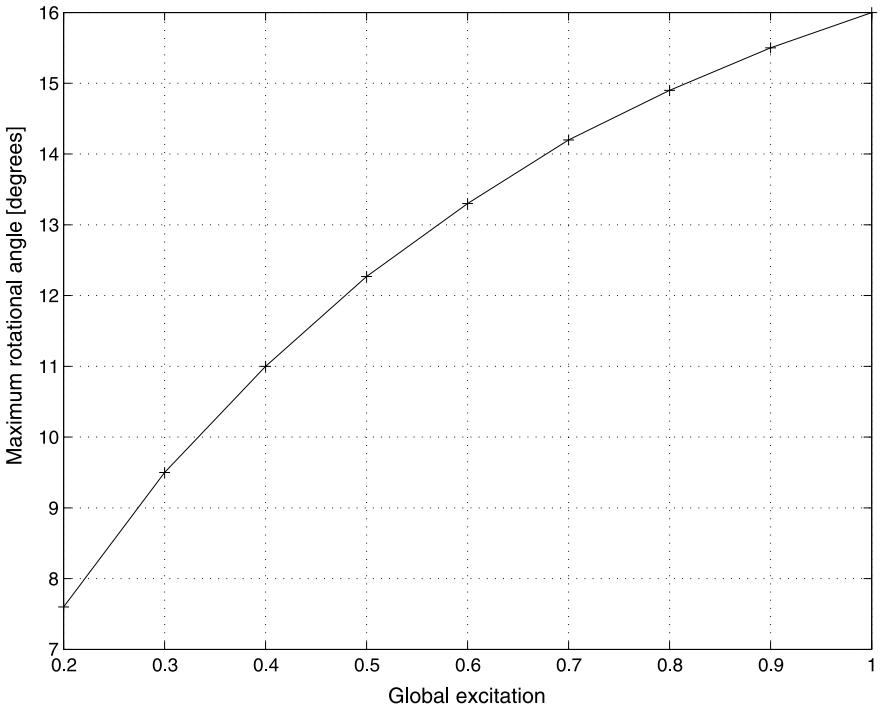

Figure 7. Effect of global excitation on the maximum rotational angle at each vertebra.

Note that to simplify the control of a belly-dancing robot in both simulation and real hardware, we tried to use the least number of body joints to imitate each posture. Interestingly, we found that except for some special postures (such as the kick and shoulder punch), the fundamental postures can be approximated by opposite movements of two joints on the same plane (Table 4). This agrees with the fact that except for the body segment required to display motions, the rest of the body torso should remain still. This is another special feature of belly dancing, which we have taken advantage of.

6 Control Architecture

After a careful analysis of belly dance movements, we found that the fundamental moves can be broken down into three types of motions: rhythmic oscillations, circular motions, and alternate contraction of muscles in two different body segments on the same plane. To mimic these movements, our proposed behavioral controller consists of three modules (Figure 10).

The first module of our controller involves a simulated lamprey central pattern generator. It generates motions that involve rhythmic oscillations (such as bending the body back and forth) as well as propagation of traveling waves along the body (as in the camel and snake arms). To generate rhythmic spine motions using the lamprey CPG, we set the global and extra excitations from the brain stem as well as the plane of motions. Since the four basic spine motions (flexion, hyperextension, lateral flexion, and twisting) as well as body undulations are planar motions, all the 3-DOF joints along the spine rotate about the same axis, and the other DOF are fixed. Thus, we only need one parameter to switch the connections between CPG outputs and motors. As a result, a total of three input parameters are adequate to control these motions. After the neural simulation is performed as described in [28], the outputs from the motor neurons are then saved into a data file for the calculation of joint angles in MATLAB. Once the plane of motions is specified, the result is used to control a simulated humanoid in Poser 5 through a script program written in PoserPython.

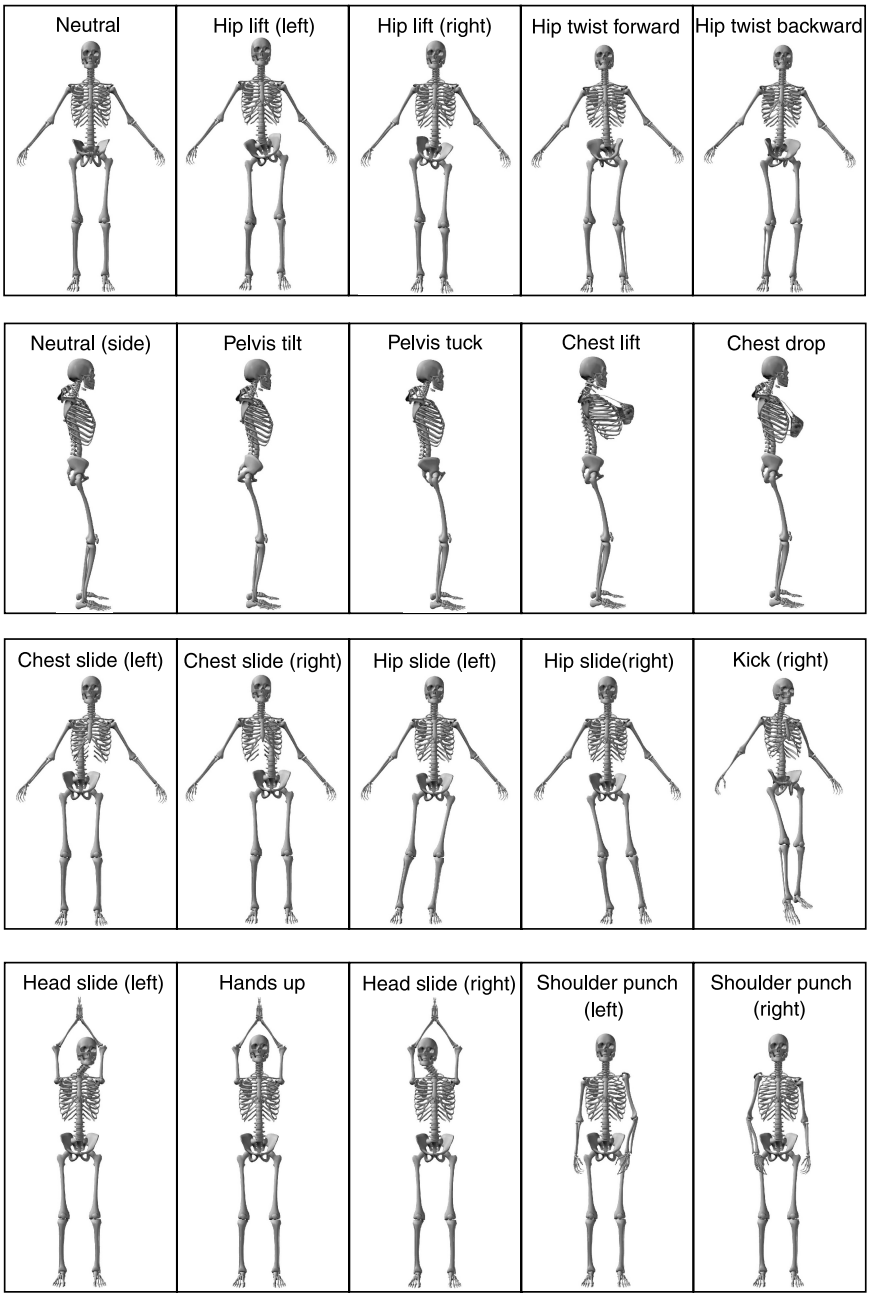

Figure 8. Fundamental dance postures commonly seen in belly dancing.

The second module of our behavioral controller is a posture database, which stores rotational joint angles required for specific postures. By sequencing these postures, dance modules such as the hip circle, vertical hip circle, hip release, hip shimmy, and shoulder shimmy can be made. Through a combination of these modules, more advanced dance moves can be achieved.

Finally, in the third module, one needs to specify the amounts of rotation and the common plane of motions of two chosen joints. It is then possible to step through the body joints in opposite directions to generate circular motions.

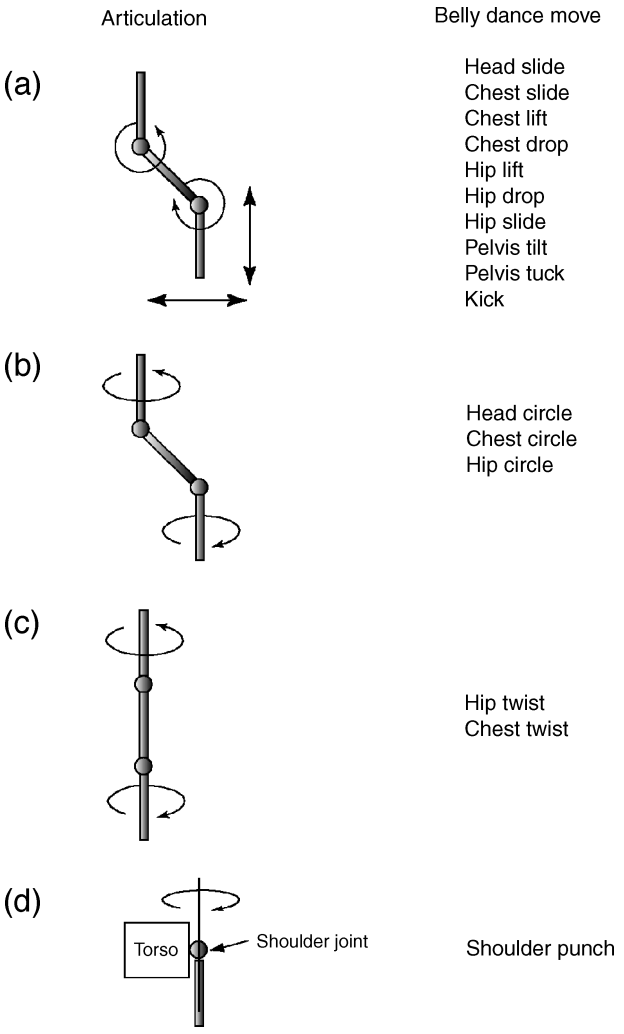

Figure 9. Functional classification of dance moves based on articulation (front view). Bars represent either the cervical, thoracic, or lumbar parts of the spine. Circles represent rotation points, places around which functional rotation would take place between the main spine segments.

7 Control of Basic Spine Motions

In this section, we investigate whether our controller is able to allow the model spine to perform all four possible actions of the human spine as defined by kinesiologists (described in Section 2.2). Note that for these motions, only three control variables are used.

7.1 Flexion

We simulated the lamprey CPG with global excitation 0.3 (out of 1.0) and no extra excitation. Without extra excitation from the brain stem to the rostral segments, the entire 100-segment CPG oscillates in phase, and a traveling wave is not generated. The effect of this is that, on specifying sagittal as the plane of motions, the simulated body bends strongly first to the front and then to the back. Body flexion is achieved (Figure 11).

Table 4. Parameters for some of the sample dance postures. The notations *xrot*, *yrot*, and *zrot* represent respectively the rotation along the *x*, *y*, and *z* axes. Note that for each posture, the rotation of one body joint is in the opposite direction to that of its counterpart. Numbers are expressed in degrees.

Posture	C7	T2	T7	L4	Hip
Hip lift (left)				−15 (side to side)	15 (*zrot*)
Pelvis tilt				−25 (bend backward)	25 (*xrot*)
Pelvis tuck				25 (bend forward)	−25 (*xrot*)
Chest lift	25 (lean forward)	−25 (lean backward)			
Chest slide (left)		−40 (side to side)	40 (side to side)		
Hip twist forward (left)				25 (twist)	−25 (*yrot*)

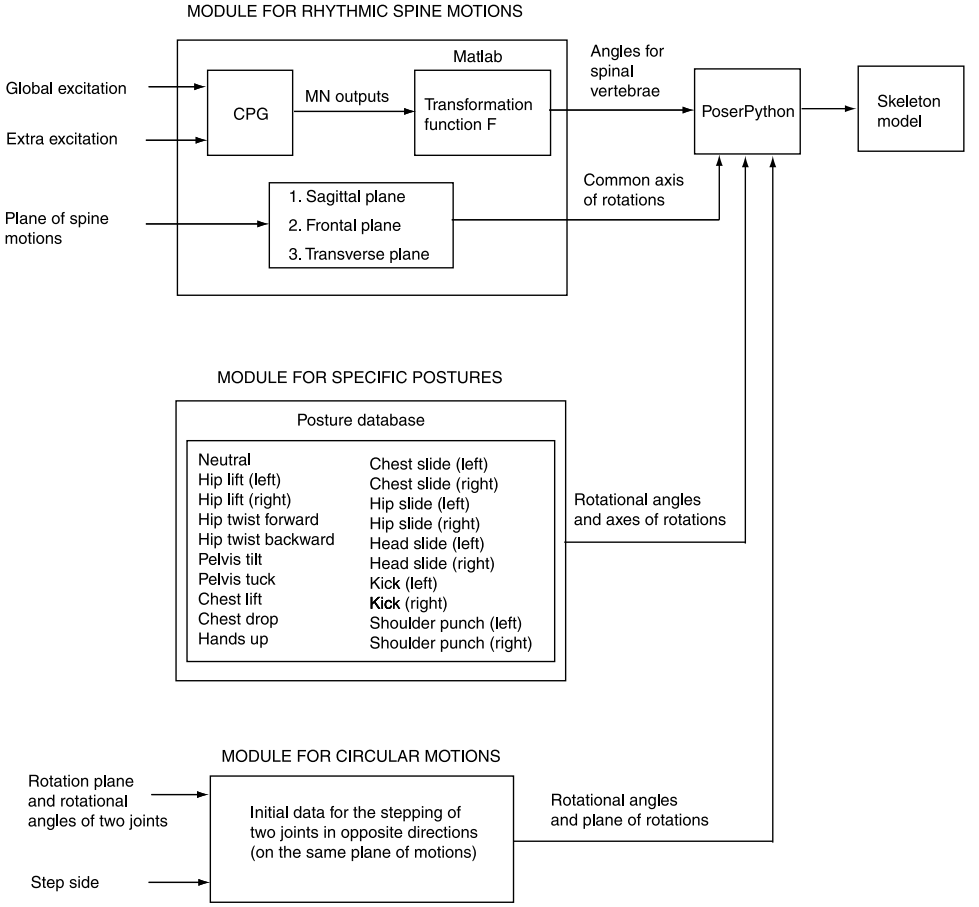

Figure 10. Schematic diagram of the behavioral controller. For the spine experiments described in this article, the transformation function *F* is the difference between the left and right motoneuron outputs amplified by a gain of 20. By sequencing the dance postures, more complicated dance movements can be accomplished.

7.2 Hyperextension

To cause the humanoid to bend more and at a higher frequency, we increased the strength of the global excitation signal to 0.7. As in the previous experiment, there is no extra excitation from the brain stem, and the plane of motions is sagittal. The stronger motoneuron outputs and higher oscillation frequency allow the humanoid to bend more and at a faster rate than that in the previous experiment. After this amplification, hyperextension results (Figure 12).

7.3 Lateral Flexion

Rather than using the motoneuron outputs to control movements on the sagittal plane, we applied the same neural wave obtained in the flexion experiment to control movements on the sides. This can be accomplished by setting the frontal plane as the plane of motion. The CPG outputs are switched to control the bending on the frontal plane. Lateral flexion is made possible (Figure 13).

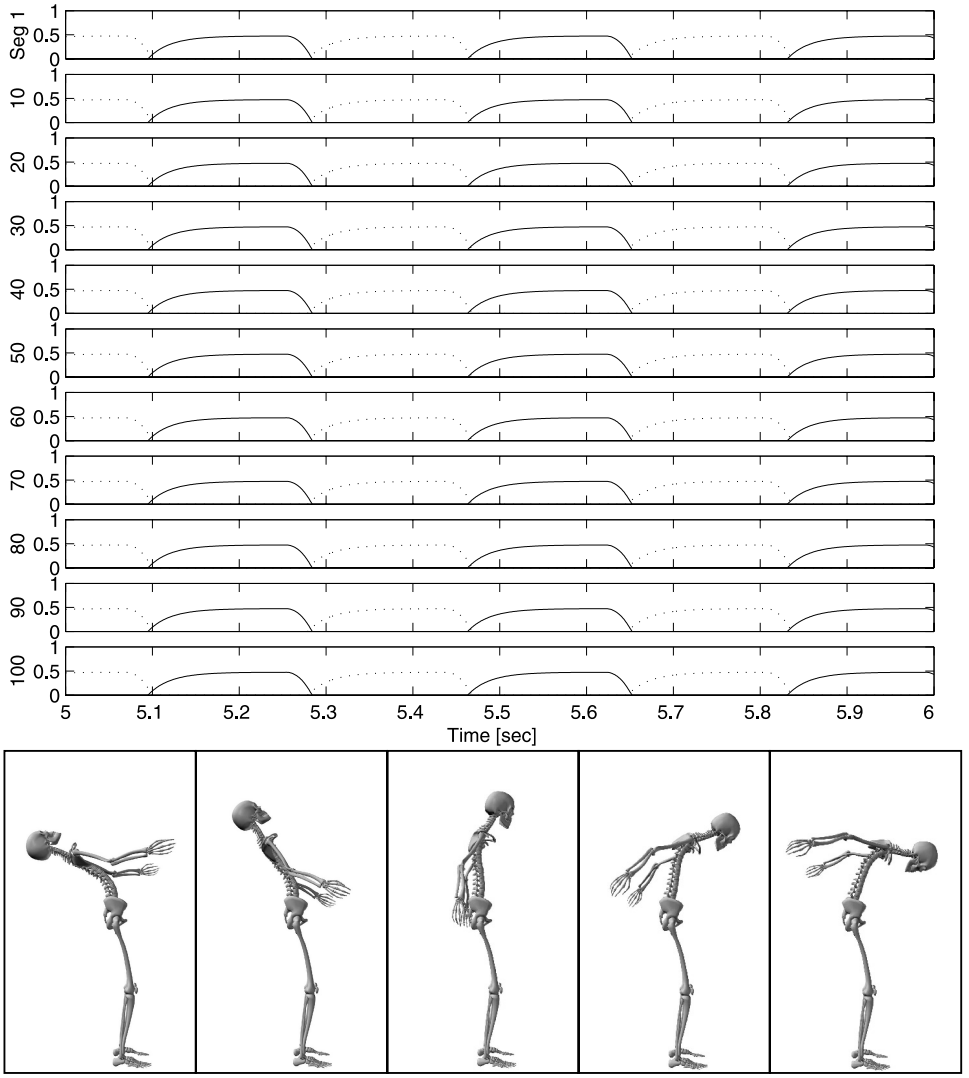

Figure 11. Neural wave generated by the lamprey CPG with global excitation 0.3 and no extra excitation. Solid lines represent the outputs from the left motoneurons, and dashed lines the outputs from the right motoneurons (*top*). Using this neural wave, the humanoid is able to achieve body flexion (*bottom*).

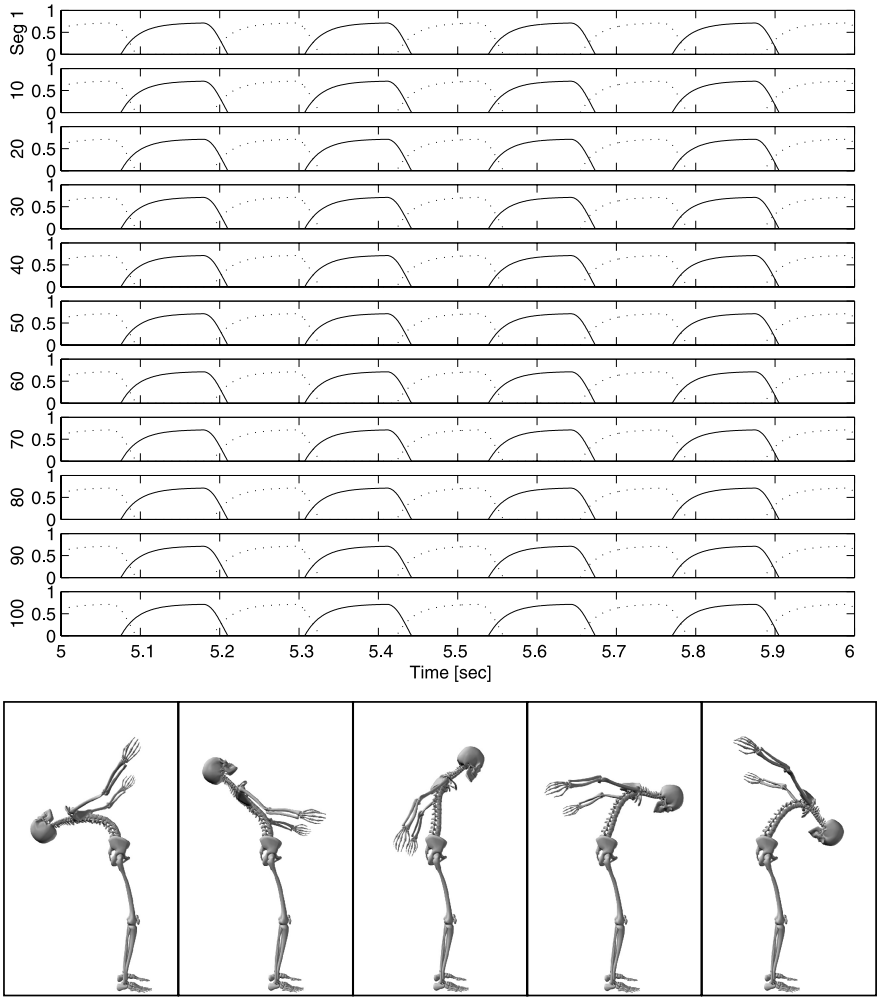

Figure 12. Neural wave generated by the lamprey CPG with global excitation 0.7 and no extra excitation. Solid lines represent the outputs from the left motoneurons, and dashed lines those from the right motoneurons (*top*). Using this neural wave, the humanoid is able to achieve hyperextension (*bottom*).

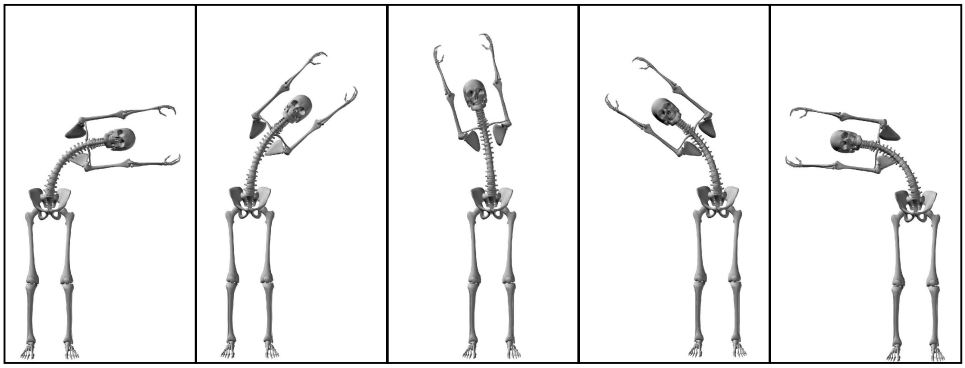

Figure 13. The humanoid is showing lateral body flexion.

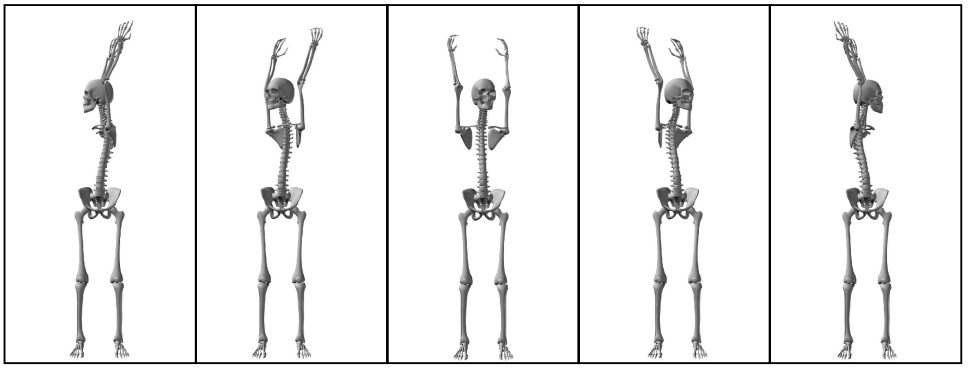

Figure 14. The humanoid is twisting its body.

7.4 Twisting

Finally, to twist the body (rotation on the transverse plane), we used the same motoneuron outputs from the flexion experiment to control the rotational angles of the corresponding spinal vertebrae. In this experiment, we chose the transverse plane as the plane of motion. The motoneuron outputs are used to control the rotations on this plane. Figure 14 shows that the body of our humanoid is able to twist.

8 Control of Complex Movements

In the previous section, we described how our model achieved basic actions of the human spine. In this section we describe how to achieve more complex belly dance movements by combining the basic postures described in Section 5. The movements we are interested in are the hip circle (transverse plane), vertical hip circle (sagittal plane), hip shimmy (frontal plane), hip release (sagittal plane), shoulder shimmy (sagittal plane), chest circle (sagittal plane), and camel (sagittal plane). These are the fundamental composite movements one has to master in order to proceed to more advanced levels. Similar to the postures in the movement database, these dance modules are the foundations for the most advanced dance moves. Since most of them are self-explanatory (Figures 15 to 19), we are describing only the chest circle and the camel here. For computer animations of the dance modules described in this article, please visit our Web site, http://www.takanishi.mech.waseda.ac.jp/jimmy/index.html.

8.1 Chest Circle

To imitate the dance move chest circle, we bend vertebrae T7 and L3 in opposite directions by 45 deg to allow the upper torso and the lower body half to be parallel (see the first move in Figure 20). Then we rotate the body joints in opposite directions on the transverse plane in steps of 36 deg. This allows the upper body torso to complete one circle in 10 steps. Note that for this dance move, no CPG is required.

8.2 Camel (Undulation)

In this experiment we set the global and extra excitations from the brain stem to 0.3 and 120% respectively. The extra excitation and intersegmental couplings cause a phase lag of 1% between successive segments along the CPG. Using the motoneuron outputs from the fifth to the sixth second to control the joint angles at each frame, a traveling wave can be made to propagate along the spine (Figure 21). This is analogous to the famous camel move.[8] Note that if we use an appropriate

8 On average, it takes 5s to complete one cycle. To mimic the dance realistically, the playback rate is set to 5.4 frames/s.

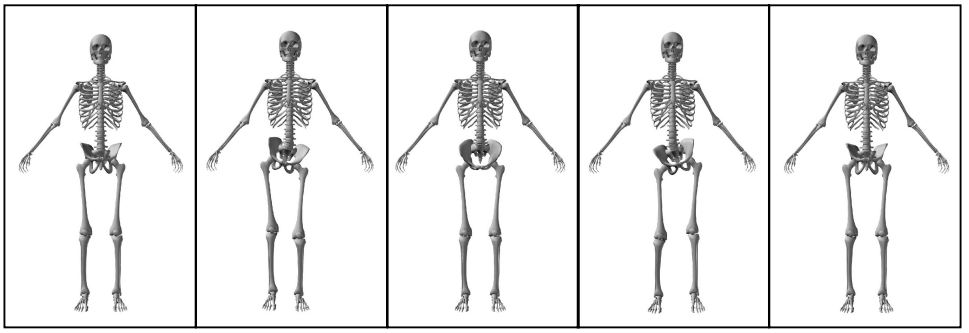

Figure 15. Hip circle. Dance sequence (*from left to right*): neutral, hip lift (right), pelvis tilt, hip lift (left), pelvis tuck, and repeat.

set of neural segments to control the joints from the shoulders to the fingers, we can produce sinusoidal motions along the arms and the hands. Movements such as the snake arms and hand ripple can be mimicked.

9 Discussion

This article presents a novel control system for a simulated, flexible spine belly-dancing humanoid robot. Using three control variables (global excitation, extra excitation, and plane of motions) for the CPG model, we are able to reproduce the four basic spine movements defined by kinesiologists as well as body undulations commonly seen in belly dancing. The CPG is particularly good at controlling rhythmic motions.

By extending the lamprey CPG, Ijspeert [17] developed a walking controller for a simulated salamander. He demonstrated that the lamprey swimming controller is robust and scalable. Although our CPG can be applied to generate rhythmic arm motions such as the snake arms and hand ripple, it is likely that it can be combined with other limb controllers such as those developed by researchers in imitation learning [3, 18, 22, 19] for the control of non-rhythmic arm movements in a real flexible spine belly-dancing humanoid robot currently under development.

From the experiments, our control system seems to be flexible. It would be interesting to apply the same controller to a different platform (such as a real robot with fewer spine segments) in order to demonstrate the adaptivity of the proposed control architecture.

When we reproduced the four basic motions of the human spine, we used the motoneuron outputs from the lamprey CPG to control every other vertebra of the simulated spine. The reason for this is that even at a global excitation of 0.3 (out of 1), the total amount of rotation from all 21

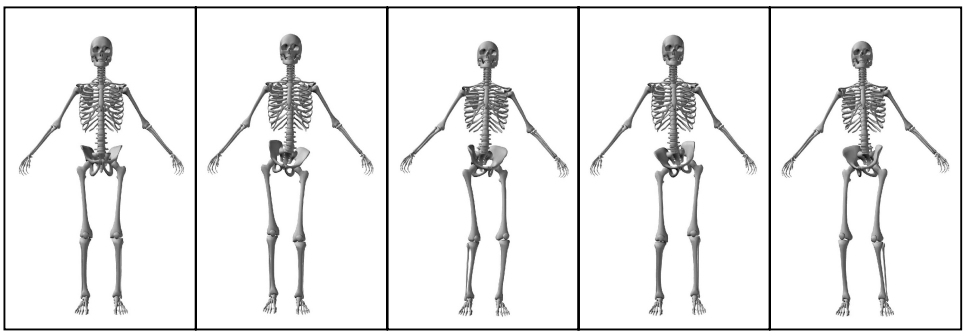

Figure 16. Vertical hip circle. Dance sequence (*from left to right*): neutral, hip lift (right), hip twist forward (right), hip drop (right), hip twist backward (right), and repeat.

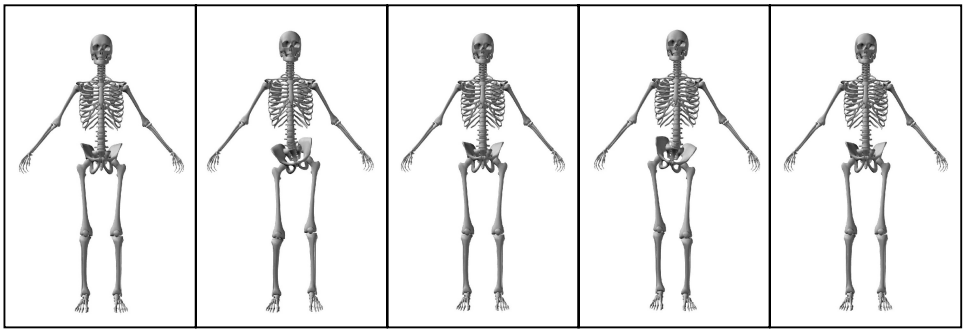

Figure 17. Hip shimmy. Dance sequence (*from left to right*): neutral, hip lift (left), hip drop (left), hip lift (right), hip drop (right), and repeat. Note that hip drop is the same as neutral.

synchronized vertebrae becomes close to 200 deg. Given that the vertebrae are interconnected and that it is less important to differentiate the action of adjacent joints in these movements, this CPG-vertebrae mapping is acceptable to generate the motions for our model humanoid. For the control of all spinal vertebrae using a wider range of control signals (the global and extra excitations), one can reduce the amplification factor involved in the calculation of joint angles. Our controller also shows flexibility in this aspect. Another benefit of controlling the spine motions using only every other vertebra is that this mapping can potentially be applied to the control of a real mechanical spine using one-third fewer motors. Thus, power consumption can be reduced.

For the experiments on using the CPG outputs to reproduce the four basic and undulation spine motions, we used one control variable to specify the plane of motion of all spinal vertebrae. Given the fact that the four basic human spine motions are planar (that is, all the joints rotate about the same axis), there might be a mechanism that controls the switching of the plane of movements even in real biological systems. This merits further investigation through collaboration with neuroscientists. Using a 3D motion capture system and comparative analysis of motions between the human belly dancer and the simulated humanoid, our work has the potential to be extended toward the biological plausibility of the proposed control scheme.

At present, our CPG-to-vertebrae mapping scheme allows the switching of connections between CPG outputs to motors about any of the three DOF axes. For nonuniform spine motions, the CPG module can easily be modified to allow specifications of this variable for each individual vertebra. Note that since some of the possible actions of the human spine are restricted by the articulation and shape of the bony landmarks, 3-DOF motions at each joint are not necessary.

In this article, we have used the motoneuron outputs from 100 evenly divided neural segments of a CPG network to control a skeleton model of 21 segments. The reason for this is that if we

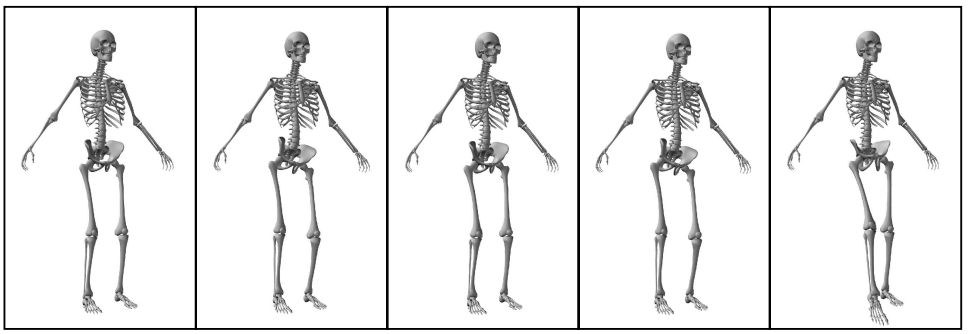

Figure 18. Hip release. Dance sequence (*from left to right*): neutral, hip lift (right), hip drop (right), hip lift (right), hip drop and kick (right), and repeat.

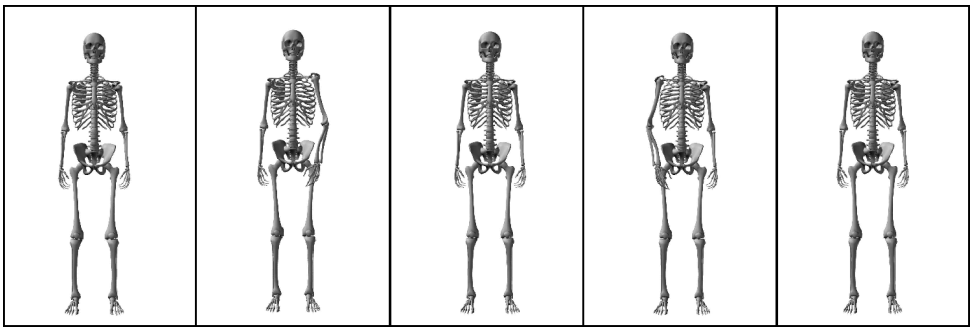

Figure 19. Shoulder shimmy. Dance sequence (*from left to right*): neutral, shoulder punch (left), neutral, shoulder punch (right), neutral, and repeat.

used the motoneuron outputs from 21 consecutive neural segments to control the vertebrae, a small intersegmental phase lag would not produce observable motions from the reduced body segments. Furthermore, since the intersegmental couplings were determined from physiological data (some neurons have connections to neurons as far as 10 segments away), shortening the CPG network by about one-fifth would change the behavior of the entire network. The special feature of relatively independent control of frequency and phase lag, as well as the regular motor patterns, would be affected.

Although the database component of our system seems to be a counterexample that shows the limitation of the CPG, it was included for simplicity and the posing of static postures. Most of the movements created by sequencing these postures can actually be generated using the CPG. For instance, all the sliding motions can be accomplished by rhythmically rotating two joints in opposite directions on the frontal plane.

Currently, our system does not have visual feedback or learning ability. It would be interesting to investigate how humans learn complex and rhythmic dance movements through observation. By

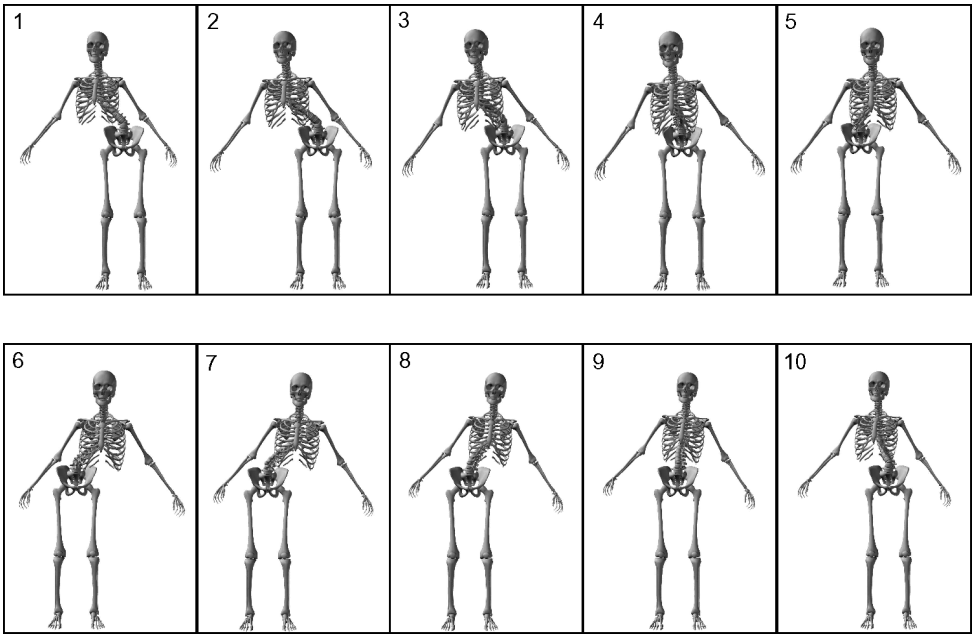

Figure 20. Chest circle.

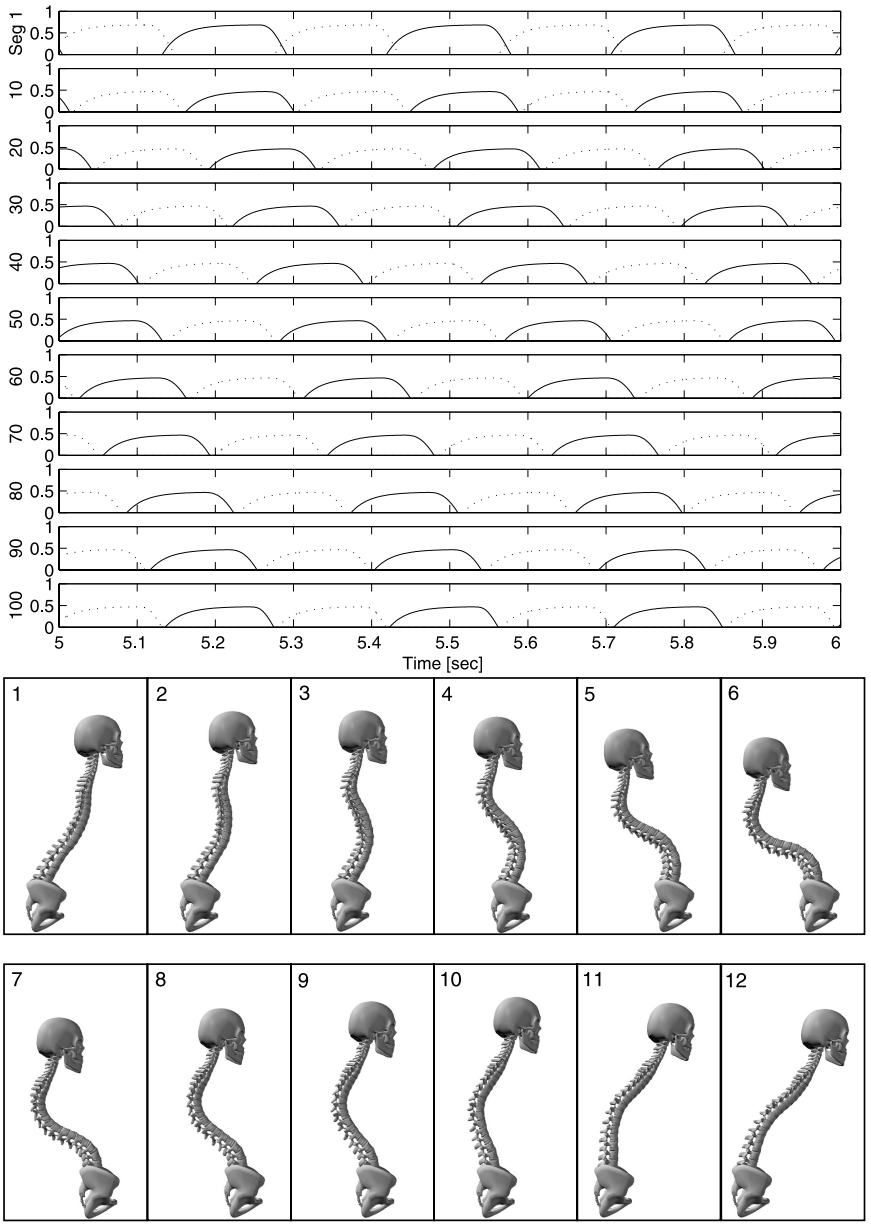

Figure 21. Neural wave generated by the lamprey CPG with global excitation 0.3 and extra excitation 120% from the brain stem. Solid lines represent outputs from the left motoneurons while dashed lines represent the outputs from the right motoneurons (*top*). Using this neural wave, the simulated humanoid is able to perform the move *camel*. For clarity, limbs are removed. Note the traveling wave along the spine.

incorporating these research findings and a visual system, it would be possible to teach a humanoid robot more complex motor behaviors by imitation learning.

Contrary to common belief, most of the movements in belly dancing are achieved through motions from the spine and/or the pelvis. Only the belly roll requires solely movements from the muscles. Due to limited resources, we used our controller to control a weightless skeleton figure in 3D animation without taking into consideration body dynamics or other physical constraints (derived from the embodiment of the human skeleton model). To implement the controller in a real

humanoid robot, factors such as gravity, weight, balancing, collisions, inertia, and elasticity need to be considered. It would be interesting to model the human skeleton and abdominal muscles using a realistic physical simulator such as the MathEngine.

Some of the frequencies of the neural waves appear to be fast for an untrained human (nearly 3 Hz in Figure 11, and about 4.5 Hz in Figure 12); the motoneuron outputs from each neural segment are actually used as a sequence of rotational commands to control the joint angles at each time frame. Within a fixed time interval (6 s for the experiments described in this article), the neural wave in Figure 11 corresponds to a slower motion than the one in Figure 12. Our approach can be applied to specify the rotational angles of real motors at each time step.

Finally, although the behaviors of CPG networks such as rhythmic oscillations and propagation of traveling waves have been reported in many articles [7, 11, 8], none has been applied to the generation of spine motions of a simulated or real humanoid robot. To the best of our knowledge, our interdisciplinary approach is the first of its kind.

10 Conclusion

This article demonstrates that by applying the control principles observed in the prototype vertebrate lamprey, it is possible to control the spine of a simulated humanoid robot. By varying the global and extra excitations from the brain stem as well as the plane of movements, the proposed lamprey CPG module could potentially generate plausible output patterns, which could be used for all the possible motions of the human spine. Furthermore, by incorporating the lamprey CPG and a posture database into our control system, the simulated humanoid robot is able to mimic the fundamental moves in belly dancing. Our work suggests that the proposed controller can potentially be applied to the control of a high-degree-of-freedom, flexible spine humanoid robot.

Acknowledgments

Many thanks for the useful comments of anonymous reviewers, Richard Stein, Lenhart Schubert, and Martin Jagersand on the earlier versions of this manuscript. The author would like to thank Lorna Gow and Alina Fischer for allowing him to attend belly dance lessons and performances. Special thanks to the professional belly dance teacher Aldiah for helping to develop the posture database.

References

1. Atéa. (2000). What is belly dance and what should we really call it? http://www.magicalmotion.com/bellydance3.htm.
2. Atkeson, C. G., Hale, J. G., Pollick, F., Riley, M., Kotosaka, S., Schaal, S., Shibata, T., Tevatia, G., Ude, A., Vijayakumar, S., & Kawato, M. (2000). Using humanoid robots to study human behavior. *IEEE Intelligent Systems*, *15*(4), 46–56.
3. Billard, A., & Matarić, M. J. (2001). Learning human arm movements by imitation: Evaluation of a biologically inspired connectionist architecture. *Robotics and Autonomous Systems*, *941*, 1–16.
4. Breazeal, C. (2002). *Designing Sociable Robots*. Cambridge, MA: MIT Press.
5. Brooks, R. A., Breazeal, C., Marjanovic, M., Scassellati, B., & Williamson, M. (1999). The Cog project: Building a humanoid robot. In C. Nehaniv (Ed.), *Computation for metaphors, analogy, and agents* (pp. 52–87). New York: Springer.
6. Chirikjian, G. (1995). A sidewinding locomotion gait for hyperredundant robots. *Advanced Robotics*, *9*(3), 195–216.
7. Delcomyn, F. (1980). Neural basis for rhythmic behaviour in animals. *Science*, *210*, 492–498.
8. Delcomyn, F. (1998). *Foundations of Neurobiology*. New York: W. H. Freeman.
9. Ekeberg, Ö. (1993). A combined neuronal and mechanical model of fish swimming. *Biological Cybernetics*, *69*, 363–374.
10. Fitt, S. S. (1988). *Dance Kinesiology*. London: Schirmer Books, a Division of Macmillan.

11. Grillner, S. (1981). Control of locomotion in bipeds, tetrapods, and fish. In V. B. Brooks (Ed.), *Handbook of physiology. Section 1. The nervous system II. Motor control* (3rd ed., pp. 1179–1236). Bethesda, MD: American Physiological Society.

12. Grillner, S. (1996). Neural networks for vertebrate locomotion. *Scientific American*, *274*(6), 48–53.

13. Grillner, S., Wallén, P., & Brodin, L. (1991). Neuronal network generating locomotor behavior in lamprey: Circuitry, transmitters, membrane properties, and simulation. *Annual Review of Neuroscience*, *14*, 169–199.

14. Grillner, S., Wallén, P., & Viana di Prisco, G. (1991). The lamprey locomotor system—Basic locomotor synergy. In M. Shimamura, S. Grillner, & V. R. Edgerton (Eds.), *Neurobiological basis of human locomotion* (pp. 77–92). Tokyo: Japan Scientific Societies Press.

15. Hashimoto, S. (2000). *Waseda University: Humanoid Robotics Institute*. Tokyo: Waseda University.

16. Iida, F., Tabata, M., & Hara, F. (1998). Generating personality character in a face robot through interaction with human. In *Proceedings of the 7th IEEE International Workshop on Robot and Human Communication* (pp. 481–486).

17. Ijspeert, A. J. (2001). A connectionist central pattern generator for the aquatic and terrestrial gaits of a simulated salamander. *Biological Cybernetics*, *84*(5), 331–348.

18. Ijspeert, A. J., Nakanishi, J., & Schaal, S. (2002). Movement imitation with nonlinear dynamical systems in humanoid robots. In *Proceedings of the IEEE International Conference on Robotics and Automation (ICRA2002)* (pp. 1398–1403).

19. Jenkins, O. C., & Matarić, M. J. (2002). Deriving action and behavior primitives from human motion data. In *Proceedings of the 2002 IEEE/RSJ International Conference on Intelligent Robots and Systems* (Vol. 3, pp. 2551–2556).

20. Kandel, E. R., Schwatz, J. H., & Jessell, T. M. (Eds.) (1985). *Principles of Neural Science* (2nd ed.). New York: Elsevier.

21. Ma, S. (2001). Analysis of creeping locomotion of a snake-like robot. *Advanced Robotics*, *15*(2), 205–224.

22. Matarić, M. (2002). Visuo-motor primitives as a basis for learning by imitation: Linking perception to action and biology to robotics. In K. Dautenhahn & C. Nehaniv (Eds.), *Imitation in animals and artifacts* (pp. 392–422). Cambridge, MA: MIT Press.

23. Miwa, H., Okuchi, T., Takanobu, H., & Takanishi, A. (2002). Development of a new human-like head robot WE-4. In *Proceedings of the 2002 IEEE/RSJ International Conference on Intelligent Robots and Systems* (Vol. 2, pp. 2443–2448).

24. Mizuuchi, I., Inaba, M., & Inoue, H. (2001). A flexible spine human-form robot—Development and control of the posture of the spine. In *Proceedings of the 2001 IEEE/RSJ International Conference on Intelligent Robots and Systems* (Vol. 3, pp. 2099–2104).

25. Mizuuchi, I., Tajima, R., Yoshikai, T., Sato, D., Nagashima, K., Inaba, M., Kuniyoshi, Y., & Inoue, H. (2002). The design and control of the flexible spine of a fully tendon-driven humanoid "Kenta." In *Proceedings of the 2002 IEEE/RSJ International Conference on Intelligent Robots and Systems* (Vol. 3, pp. 2527–2532).

26. Nakazawa, A., Nakaoka, S., Ikeuchi, K., & Yokoi, K. (2002). Imitating human dance motions through motion structure analysis. In *Proceedings of the 2002 IEEE/RSJ International Conference on Intelligent Robots and Systems* (Vol. 3, pp. 2539–2544).

27. Nugent, M. (2000). Bellydance movement vocabulary. http://www.venusbellydance.com/vocabulary.htm.

28. Or, J. (2002). *An investigation of artificially-evolved robust and efficient connectionist swimming controllers for a simulated lamprey*. Ph.D. thesis, University of Edinburgh, Edinburgh.

29. Sakagami, Y., Watanabe, R., Aoyama, C., Matsunaga, S., Higaki, N., & Fujimura, K. (2002). The intelligent ASIMO: System overview and integration. In *Proceedings of the 2002 IEEE/RSJ International Conference on Intelligent Robots and Systems* (Vol. 3, pp. 2478–2483).

30. Sarrigeorgidis, K. (1999). The NTUA snake; Design, planar, kinematics, and motion planning. *Journal of Robotic Systems*, *16*(1), 37–72.

31. Shan, J., & Nagashima, F. (2002). Neural locomotion controller design and implementation for humanoid robot HOAP-1. In *20th Annual Conference of the Robotics Society of Japan* (presentation 1C34). Robotics Society of Japan.

32. Yamasaki, F., Endo, K., Asada, M., & Kitano, H. (2002). An energy-efficient walking for a low-cost humanoid robot PINO. *AI Magazine*, *23*(1), 60–61.